ELSEVIER

Food Chemistry 76 (2002) 89–102

Food Chemistry

www.elsevier.com/locate/foodchem

Analytical, Nutritional and Clinical Methods Section

Differential scanning calorimetric analysis of palm oil, palm oil based products and coconut oil: effects of scanning rate variation

C.P. Tan, Y.B. Che Man*

Department of Food Technology, Faculty of Food Science and Biotechnology, Universiti Putra Malaysia, 43400 UPM Serdang, Selangor D.E., Malaysia

Received 16 January 2001; received in revised form 21 May 2001; accepted 21 May 2001

Abstract

This study explored the thermal behaviour of coconut oil and palm oil and products based on them, by monitoring peak transition temperatures, transition enthalpies, offset- (T_{off}) and onset-temperatures (T_{on}) by differential scanning calorimetry (DSC) at different scanning rates. Triacylglycerol (TAG) profiles and iodine value (IV) analyses were used to compliment the DSC data. An increase in heating rate, generally, was associated with an increase in peak size, peak transition and offset temperatures. Meanwhile, the peak transition and onset temperatures increased with decreasing cooling rates. Decreased heating or cooling rate also caused a narrowing of the melting endotherms or crystallisation exotherms. Transitions for oil samples with low scanning rate (1 °C/min) were composed of more peaks, resulting from the contribution of a number of TAG components in the oil. Generally, coconut oils and palm-based products may be differentiated with their T_{off} and T_{on} values in the DSC melting and crystallisation curves, respectively. On the basis of the results of this study, DSC can provide information about the nature of TAG interaction in these oil samples. Recognition of the pattern of interactions among TAG in coconut- and palm-based products can be helpful in many physical processes in the palm oil industry.

Keywords: Coconut oil; Differential scanning calorimetry; Palm oil; Thermal behaviour

1. Introduction

Palm oil and coconut oil (CtO) are two of the most important oil crops in tropical regions. Therefore, an understanding of the thermal behaviour of these edible oil products is important for many practical applications in the oils and fats industry. Over the past two decades, differential scanning calorimetry (DSC) has been increasingly utilised for thermodynamic characterisation of edible oils and fats (Dollimore, 1996). The rapid growth in popularity can be attributed in part to the availability of instruments of higher sensitivity and greater ease-of-use, as well as to software which provides rigorous analysis of experimental data, even for the non-expert (Ma, Harwalkar, & Maurice, 1990). Recently, DSC has been used to monitor the degree of oxidation and quantitative determination of total polar compounds in heated oils (Tan & Che Man, 1999a, 1999b).

Generally, edible oils and fats are long-chain compounds that have particular properties of importance in processing and final use. For investigation of edible oils and fats at temperatures between −100 °C and 80 °C, many different thermal behaviours can be observed (Tan & Che Man, 2000). The most important aspect of the physical properties of oils and fats is related to the solid–liquid and liquid–solid phase changes; in other words, melting and crystallisation. Crystallisation of liquid oil results in a volume contraction and a positive (exothermic) heat effect. Melting of a fat results in volume expansion and a negative (endothermic) heat effect.

It is well known that melting and crystallisation behaviours of edible oils and fats are two of the important properties for functionality in many prepared food products. These thermal properties are counterparts of the triacylglycerol (TAG) profile in edible oils and fats (Breitschuh & Windhab, 1996). Melting and crystallisation can both be measured by DSC. They may be either endothermic or exothermic processes. In general,

* Corresponding author. Tel.: +60-3-8948-6101, ext. 3468; fax: +60-3-8942-3552.

E-mail address: yaakub@fsb.upm.edu.my (Y.B. Che Man).

0308-8146/01/$ - see front matter
PII: S0308-8146(01)00241-2

oils and fats can exhibit extremely complex thermal behaviour (Tan & Che Man, 2000), which will be highly dependent on the detailed chemical composition and protocol for the DSC experiment. It is therefore difficult to describe the thermal behaviour of a complex oil or fat system, such as palm oil and palm-based products, in any general way. Nonetheless, in principle, the thermal profile of edible oils and fats contains a great deal of information regarding the nature of the transition and can serve as a very useful probe for "fingerprinting" a given oil or fat (Tan & Che Man, 2000). An early review showed that many systematic works have been published on pure TAG as model systems (Cebula & Smith, 1991; Sato, 1999).

Since the pioneering works in modern thermal analysis were published, it has been well known that scanning rate has a strong effect on the thermal profile of a given substance (Herrera, Segura, Rivarola & Añón, 1992). However, this effect is neglected in most studies. To the best of our knowledge, analysis of the effect scanning rate is scarce for palm-based and coconut products. Establishing the effects of scanning rate on DSC characteristics is critical to qualitative or quantitative analyses of these products. Therefore, two general goals of this work are to test the applicability of the DSC procedure for dynamic experiments, as taken place in calorimetric analysis of CtO and palm oil and palm-based products, and to correlate thermal characteristics with chemical composition of these products. This paper reports detailed DSC investigation in four different scanning rates, coupled with chemical constituent investigation. It describes experimental methods and introduces parameters and variables to be considered in such dynamic experiments.

2. Materials and methods

2.1. Materials

Six different palm oil and palm-based products were used in this study. Refined-bleached-deodorised palm oil (RBDPO), refined-bleached-deodorised palm stearin ($RBDPO_s$), and palm kernel oil (PKO) were obtained from a local refinery. The other samples were purchased from several local retailers. All chemicals and solvents used were Analar or HPLC grades (Merck, Darmstadt, Germany). Fatty acid methyl esters (FAME) and TAG standards were obtained from Sigma Chemical Co (St. Louis, MO, USA).

2.2. Iodine value analysis

The AOCS Official Method was employed for determinations of iodine value (IV) in the oil samples (AOCS, 1993).

2.3. TAG analysis by HPLC

HPLC analysis was performed as described previously for edible oils (Tan & Che Man, 2000). TAGs were separated according to their degree of unsaturation and molecular weight. TAG peaks were identified, based on the retention time of TAG standards. The TAG data were treated as percentage areas. Separated TAG peaks, with an area below 0.1%, were not integrated. The quantification was carried out by normalisation. Each sample was chromatographed three times and the data were reported as percent areas.

2.4. Thermal analysis by DSC

For DSC analysis, a Perkin–Elmer differential scanning calorimeter, DSC-7 equipped with a thermal analysis data station (Perkin–Elmer Corp., Norwalk, CT, USA) was used. Nitrogen (99.999% purity) was the purge gas and flowed at approximately 20 ml/min. The calorimeter was calibrated according to standard procedures established in the manufacturer user manual. The DSC instrument was calibrated using indium (m.p. 156.6 °C, $\Delta H_{f=}28.45$ J/g) and *n*-dodecane (m.p. −9.65 °C, $\Delta H_{f=}216.73$ J/g). For each scanning rate, the calibration procedure was completed with the same scanning rate. Samples of ca. 6–12 mg were weighed into aluminium pans (inner volume: ca. 20 ml) to the nearest 0.1 mg, and covers were hermetically sealed into place. An empty, hermetically sealed aluminium pan was used as reference. Prior to analysis of samples, the baseline was obtained with an empty, hermetically sealed aluminium pan. Samples were subjected to the following temperature programme: 80 °C isotherm for 5 min, cooled to −80 °C and held for 5 min. The same sample was then heated from −80 to 80 °C. In the present study, the samples were cooled and/or heated at four predetermined scanning rates, namely 1, 5, 10, and 20 °C/min. Each DSC scan was collected on a new sample to ensure that all of the samples started with the same thermal history and "standard" state.

The manufacturer's software (7 Series/UNIX DSC software library) programme was used to analyse and plot the thermal data (Anon, 1995). An effort was made to have all samples of the same weight but the weights were not identical; therefore, the DSC scans shown in all figures have been normalised to account for the small sample weight variation. The thermal melting and crystallisation characteristics of each sample in a DSC scan can be indicated by various temperatures. The melting transition temperatures were assigned to each thermal curve, based on the temperature at which the greatest value for the heat flow occurred, while the crystallising transition temperatures were assigned to each thermal curve, based on the temperature at which the lowest value for the heat flow occurred. For the melting curve,

the offset-temperature (T_{off}; point where the extrapolated leading edge of the last endotherm intersects with the baseline) was also determined (Fig. 1). The start of crystallisation transition, T_{on}, for all studies, was taken as the onset point of the transition, that is the point at which the extrapolated baseline intersects the extrapolated slop in the transition state (Fig. 1). The onset- and offset-temperatures could not be determined from the melting and crystallisation curves, respectively, because no final baseline was observed. In the study, only peak enthalpies (in joule per gramme), at 1 °C/min, were determined, as in many cases it was difficult to define a pre-peak baseline, and furthermore, the baseline slope for some of the melting or crystallisation curves appeared to change over the course of the scan and may not be horizontal. All DSC values reported are the average of four scans.

2.5. Statistical analyses

Data were statistically analysed by one-way analysis of variance (ANOVA) with the SAS software package (SAS Institute, Cary, NC, USA, 1989). Duncan's multiple-range test was applied to determine significant differences between means, at a level of $P < 0.01$.

3. Results and discussion

3.1. General

In the present study, the effect of heating rates on melting curves of oil samples was determined by DSC analysis as shown in Figs. 2–7. All DSC melting data are summarised in Table 2. Figs. 8–13 illustrate the crystallisation curves of oil samples at four different cooling rates, and Table 3 lists their respective exothermic temperatures. For reference, the melting and crystallisation curves have been labelled with A, B, C, and D for scanning rates at 1, 5, 10, and 20 °C/min, respectively. The endotherms in each melting curve have been labelled in order of increasing temperature, while the exotherms in each crystallisation curve have been marked in order of decreasing temperature. The IVs of all oil samples are tabulated in Table 1. The TAG compositions of the six oil samples are shown in Table 4, while the proportion of trisaturated (SSS), disaturated–monounsaturated (SSU), monosaturated–diunsaturated (SUU) and triunsaturated (UUU) TAG data are tabulated in Table 5.

Considering the complexity of the thermal behaviour of each oil sample, the identification and interpretation of their thermal events were approached with caution. Similarities between certain oil samples were evident (e.g. CtO and PKO; $RBDPO_{SO}$ and RPO_O), yet in many ways each oil sample was unique. Therefore, a thorough study of their melting and crystallisation

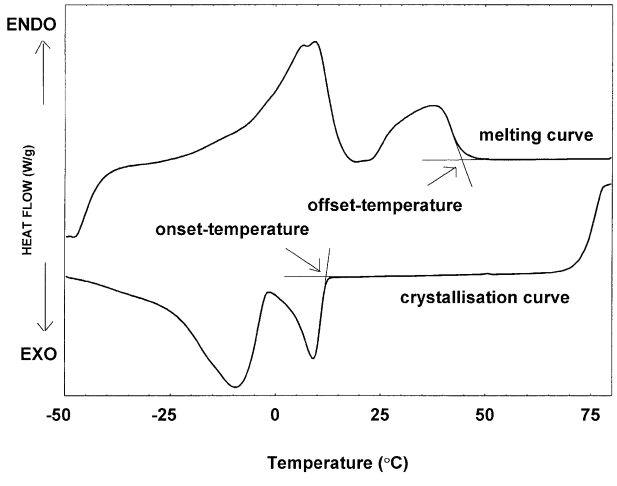

Fig. 1. Differential scanning calorimetry (DSC) melting and crystallisation curves of refined-bleached-deodorised palm oil (RBDPO) at scanning rate of 20 °C/min. The techniques used for determination of the DSC parameters are illustrated by constructed lines. The onset- and offset temperatures corresponded closely to the intersection of the extrapolated baseline and the tangent line (leading edge) of the peak.

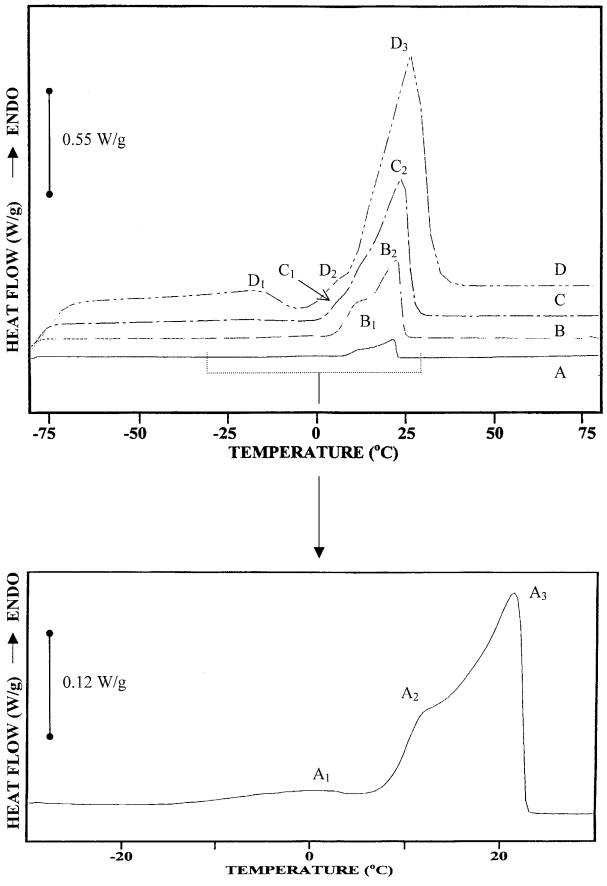

Fig. 2. Differential scanning calorimetry melting curves of coconut oil (CtO) at heatinf rates varying from 1 to 20 °C/min. Abbreviations: A, 1 °C/min; B, 5 °C/min; C, 10 °C/min; D, 20 °C/min. Refer to Table 2 for transition temperatures.

behaviours can be useful for identification of each oil sample and for monitoring physical processes in the oils and fats industry, such as the fractionation process.

3.2. Behaviour of oils during the heating process

The results of the present study reveal that the transition temperatures and peak shapes in DSC melting curves of oil samples are dependent on the scanning rate. The relative magnitude and temperature of the peak increases as heating rate is increased. High scanning rates result in high melting points, owing to the poor oil thermal conductivity: at high scanning rates, there is no time for the heat to be transmitted from the heating elements of the DSC cell to the sample. Therefore, a peak transition temperature at a heating rate of 20 °C/min may be higher than the value obtained by lower heating rates. Moreover, at increased heating rates, the shape of the melting curve is smoothed and, as a result, detailed information may get lost. The number of peaks in the heating curves is also dependent on the scanning rate. The changes of DSC profile with heating

Table 1
Edible oil samples and their iodine values (g of I_2/ 100g oil) used in this study

Sample identification	Abbreviation	Iodine value
Coconut oil	CtO	9.37±0.19
Palm kernel oil	PKO	19.3±0.01
Refined-bleached-deodorised palm oil	RBDPO	53.8±0.19
Refined-bleached-deodorised palm stearin	$RBDPO_S$	32.8±0.28
Refined-bleached-deodorised palm superolein	$RBDPO_{SO}$	61.9±0.01
Red palm olein	RPO_O	65.0±0.39

Table 2
Comparison of differential scanning calorimetry-measured transition temperatures for four different heating rates of edible oil samples[a]

Sample	Rate (°C/min)	Transition temperature (°C)[b]						
		1	2	3	4	5	6	7
CtO	1	0.83	11.31	21.05				
	5	−2.64	12.42	22.45				
	10	7.87	23.63					
	20	−16.67	6.26	26.33				
PKO	1	−4.86	1.25	16.76	24.02			
	5	−19.12	1.31	13.13	26.03			
	10	−19.37	2.13	15.03	27.93			
	20	−13.80	32.06					
RBDPO	1	−20.70	−8.16	−5.52	0.92	10.82	26.82	41.51
	5	−18.40	−6.22	0.23	5.25	21.91	35.35	
	10	−16.5	−5.03	2.85	6.43	27.22	35.82	
	20	−13.8	9.13	37.80				
$RBDPO_{SO}$	1	−19.22	−12.29	−3.05	0.59	5.54	9.99	
	5	−38.47	−28.43	−15.53	−4.78	3.82	8.12	
	10	−39.43	6.43	9.30				
	20	−36.74	−16.67	9.13				
$RBDPO_S$	1	12.96	18.24	39.69	47.12	53.22		
	5	−18.40	−6.93	0.95	6.68	29.62	37.50	55.06
	10	−17.93	2.13	9.30	33.67	44.42	56.60	
	20	−13.80	12.00	53.57				
RPO_O	1	−18.72	−7.01	−1.23	1.41	4.71	7.68	13.95
	5	−41.33	−32.73	−12.67	−5.50	2.38	4.18	
	10	−39.43	−9.33	2.85				
	20	−36.74	−16.67	6.26				

[a] Each value in the table represent the mean for four determinations. Standard deviations of the reported results are in the range of 0–0.93 °C, 0–1.56 °C, 0–2.33 °C, 0–0.99 °C for 1, 5, 10, and 20 °C/min, respectively.
[b] Based on indicators A, B, C, and D in Figs. 2–7. Abbreviations: see Table 1.

rate are complicated; some profiles have more than six endothermic peaks, while other curves with higher rates show only three endothermic peaks (Figs. 4–6). However, this is useful in considering the change of the different endotherms with various heating rates. All DSC melting transition temperatures quoted refer to maximum peak temperatures.

When heated in a differential scanning calorimeter (DSC), oil samples often exhibit multiple endotherms. Multiple endothermic peaks are quite commonly observed in DSC. Although there are undoubtedly a variety of reasons for this phenomenon, two major causes predominate. One of these results from a consequence of unique features in the TAG distribution. The unique features of TAG present in vegetable oils are the main building block for their application in the food industry. Generally, the highly saturated TAG (SSS) melted at higher temperatures than the highly unsaturated TAG (UUU), with the SSU and SUU TAG melting in between these two extremes. The other is the melting-recrystallisation of the original TAG crystallites and their subsequent melting known as the polymorpism phenomenon. Although these observations are of interest by themselves, they become particularly important when the endothermic peaks are being used to establish the thermodynamic properties of the initial fat crystallites. Nevertheless, there is no obvious way to determine the origin of the multiple peaks by just examining the melting curves.

DSC peak analysis allows the determination of the temperature of transition of a given oil or fat. The heating rate affects the sharpness of the peaks in the DSC endotherm of the oils. The sharpness of the peak also indicates the cooperative nature of the transition from TAG composition. If transition occurs in a very narrow range of temperatures, it is highly cooperative. Evidence has already been provided that melting of TAG complexes can occur simultaneously during heating in the DSC (Tan & Che Man, 2000). Therefore, in a certain temperature range, melting of the two or more TAG structures could take place simultaneously, resulting in broad or overlapping melting transitions. In our studies, the endothermic processes were more pronounced in

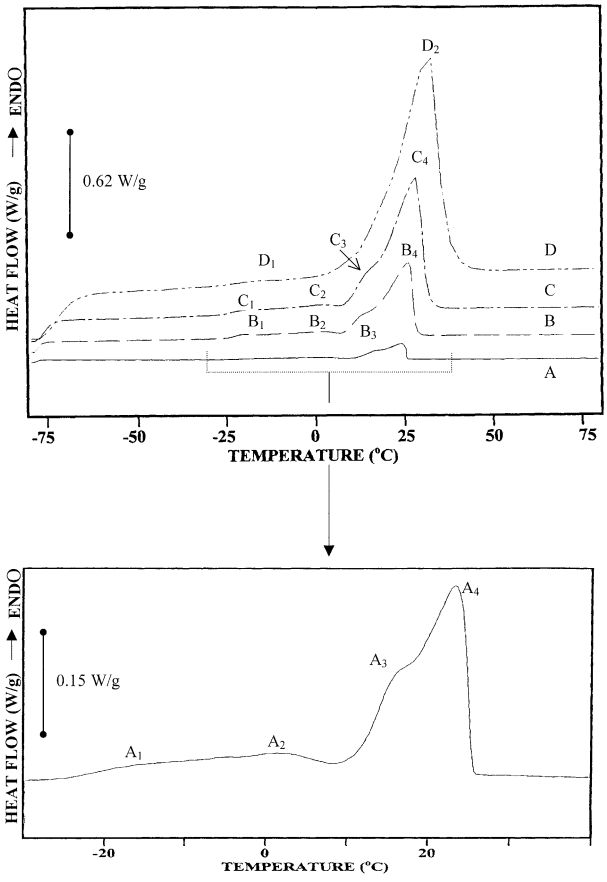

Fig. 3. Differential scanning calorimetry melting curves of palm kernel oil (PKO) at heating rates varying from 1 to 20 °C/min. Abbreviations: see Fig. 2. Refer to Table 2 for transition temperatures.

Table 3
Comparison of differential scanning calorimetry-measured transition temperatures for four different cooling rates of edible oil samples[a]

Sample	Rate (°C/min)	Transition temperature (°C)[b]					
		1	2	3	4	5	6
CtO	1	2.71	0.74				
	5	−0.70	−7.86				
	10	−2.87	−16.49				
	20	−8.27	−25.47				
PKO	1	7.83	6.17	3.87			
	5	−1.09	−2.49				
	10	−2.16	−8.61				
	20	−5.40	−19.73				
RBDPO	1	18.39	0.74	−8.68	−22.70	−33.10	−37.38
	5	15.43	6.11	−2.85	−11.09	−46.92	
	10	12.89	−5.74	−12.91	−56.63		
	20	8.93	−11.13	−68.47			
$RBDPO_{SO}$	1	0.07	−7.36	−23.25	−40.52		
	5	−2.85	−8.94	−28.29	−56.95		
	10	−6.46	−30.11	−63.07			
	20	−11.13	−35.50	−71.33			
$RBDPO_S$	1	29.94	9.47	−2.08	−16.93		
	5	27.25	−1.41	−11.09			
	10	24.36	−4.30	−28.67			
	20	18.97	−9.70				
RPO_O	1	−1.25	−7.52	−26.33	−42.83		
	5	−3.92	−27.57	−60.54			
	10	−8.61	−30.11	−64.50			
	20	−14.00	−34.07	−74.20			

[a] Each value in the table represent the mean for four determinations. Standard deviations of the reported results are in the range of 0–1.09 °C, 0–1.94 °C, 0–1.56 °C, 0–2.65 °C for 1, 5, 10, and 20 °C/min, respectively.

[b] Based on indicators A, B, C, and D in Figs. 8–13. Abbreviations: see Table 1.

melting curves with increased rates of heating; however, the features were similar as far as the major transition peaks were concerned.

TAG have the property that they are able to exist in several crystalline structures or polymorphic forms (Desmedi, Culot, Deroanne, Durant, & Gibon, 1990). As the oil samples are heated, some of the less thermally-stable polymorphs melt; the remaining TAG rearrange, and recrystallise into more stable polymorphs that melt at higher temperatures. However, in the field of oils and fats, an exotherm associated with the recrystallisation may or may not be exhibited in DSC melting curves. The exothermic changes that appear below the baseline are a measure of the transition and crystallization to a higher melting polymorph. On the other hand, when a partial melting of a polymorph, accompanied by a conversion or transition to a higher polymorph takes place, both endothermic peak and endothermic changes are represented in a single endothermic peak. Therefore, thermal behaviour interpretations, based on such DSC scans, must be made with caution. The crux of the present study is whether sufficient material is recrystallised to a more stable polymorph during the course of thermal analysis and recorded in the DSC scan of the oil samples. We hypothesized that, when there is a small amount of recrystallisation, the sum of the enthalpy changes associated with melting and recrystallisation may be positive or zero at all temperatures, and no exotherm will be detectable in the DSC scan. For larger amounts of recrystallisation, the sum may become negative, and an exotherm will be displayed. The amount of recrystallisation depends on the stability of the original crystal population, which will depend on its crystallisation history, and on the amount of time the sequences have for rearrangement and recrystallisation, which will depend on the heating rate. Unlike pure TAG, the type polymorphic form of a given edible oils cannot be established unequivocally by DSC (deMan & deMan, 1994). This can only be achieved by X-ray diffraction analysis.

In favourable cases with $RBDPO_S$, the melting of the initial fat crystallites, their recrystallisation, and their subsequent melting were resolved by DSC (Fig. 5). A continuous crystallisation exotherm at temperatures between the two major melting endotherms was observed for the $RBDPO_S$ sample, and this exotherm

Table 4
Comparison of triacylglycerol (TAG) composition (area%) among edible oil samples[a]

TAG	Sample (Group 1)					
	CtO	PKO	RBDPO	$RBDPO_S$	$RBDPO_{SO}$	RPO_O
CCLa	12.9±0.2	6.8±0.0				
CLaLa	17.4±0.2	9.9±0.0				
LaLaLa	21.2±0.3	21.2±0.2				
LaLaM	18.0±0.3	17.0±0.0				
LaLaO	3.1±0.0	5.3±0.0				
LaMM	10.2±0.1	8.8±0.0				
MMM			0.4±0.0	0.2±0.0	0.7±0.0	0.6±0.0
LaLaP	0.5±0.0	1.2±0.0				
LaMO	2.4±0.1	4.6±0.0				
MPL			2.4±0.1	1.0±0.2	3.2±0.0	3.7±0.1
LaMP	5.5±0.1	4.6±0.0				
LaOO	1.1±0.0	3.8±0.0				
LaPO	1.6±0.2	4.3±0.0				
LaPP + MMO	2.1±0.3	1.9±0.0				
OOL			0.7±0.0	0.1±0.0	0.7±0.0	0.8±0.1
MMP	0.2±0.0	0.7±0.1	1.8±0.1	0.8±0.1	2.3±0.1	2.6±0.1
MOO	0.8±0.1	2.0±0.0				
MPO + POL	1.1±0.0	2.1±0.0				
POL			10.1±0.0	5.3±0.5	12.8±0.0	15.8±0.1
PPL		0.6±0.1	9.8±0.1	7.8±0.0	10.7±0.0	11.2±0.0
MPP			0.6±0.0	2.3±0.0		
OOO	0.6±0.1	1.4±0.0	4.1±0.0	1.8±0.0	4.9±0.0	5.6±0.0
POO	0.3±0.0	1.9±0.1	24.2±0.1	12.0±0.2	29.1±0.0	36.3±0.0
PPO	0.7±0.1	1.1±0.1	31.1±0.1	29.8±0.0	27.2±0.1	17.1±0.1
PPP	0.6±0.1	0.1±0.0	5.9±0.0	29.2±0.2		0.1±0.0
SOO		0.4±0.1	2.3±0.1	0.8±0.1	3.1±0.1	3.6±0.0
PSO		0.4±0.1	5.1±0.0	3.8±0.0	5.0±0.1	2.5±0.1
PPS			0.9±0.0	5.2±0.2		
SSO			0.5±0.0		0.4±0.1	

[a] Each value in the table represents the mean standard deviation of triplicate analyses. Abbreviations: TAG, triacylglycerol; C, capric; La, lauric; M, myristic; P, palmitic; S, stearic; O, oleic; L, linoleic. For other abbreviations see Table 1.

reflects polymorphic changes. Since each endotherm is produced by the melting of an individual or a group of TAG crystal populations formed during heating of the oil samples in the calorimeter, polymorpism phenomena would create a significant effect on the melting endotherm, before or after the reorganisation process. Therefore, for each of pre- and post-reorganisation, respective endotherms do not represent the properties of the original crystallite. Their use in thermodynamic analysis results in considerable error.

3.2.1. Coconut oil (CtO)

The DSC heating curves for CtO and their corresponding transition temperatures, at a series of heating rates are illustrated in Fig. 2 and Table 2. All melting endotherms were similarly evident at all the heating rates. Only one major heating endotherm was present with one/two slight shoulders on the lower temperature side (Fig. 2, curves A–C). We believe that this major endotherm peak was the melting peak of five major trisaturated SSS TAG present in CtO, namely CCLa, CLaLa, LaLaLa, LaLaM, and LaMM, which accounted for almost 80% of the total TAG. As the heating rate was increased, the shoulders moved to lower temperatures. In addition, an apparent splitting of the lower-temperature endotherm occurred with the main peak first appearing when the heating rate was at 20 °C/min (Fig. 2, curve D). Consequently, with this split effect, careful inspection of the melting curves of the CtO revealed a broad exothermic region between the D_1 and D_2.

3.2.2. Palm kernel oil (PKO)

The variation of DSC profile and corresponding transition temperatures of PKO are shown in Fig. 3 and Table 2. In general, the melting endotherms in PKO showed little changes in either the peak temperatures or the shape. This is probably due to the presence of large SSS TAG groups (CCLa, CLaLa, LaLaLa, LaLaM, and LaMM) which mainly consist of medium chain fatty acid. These TAG groups were considered stable against changes in heating rate variation. The melting curves of PKO displayed one prominent peak with a large, lower-temperature shoulder peak and two other small, contiguous lower-temperature endotherms.

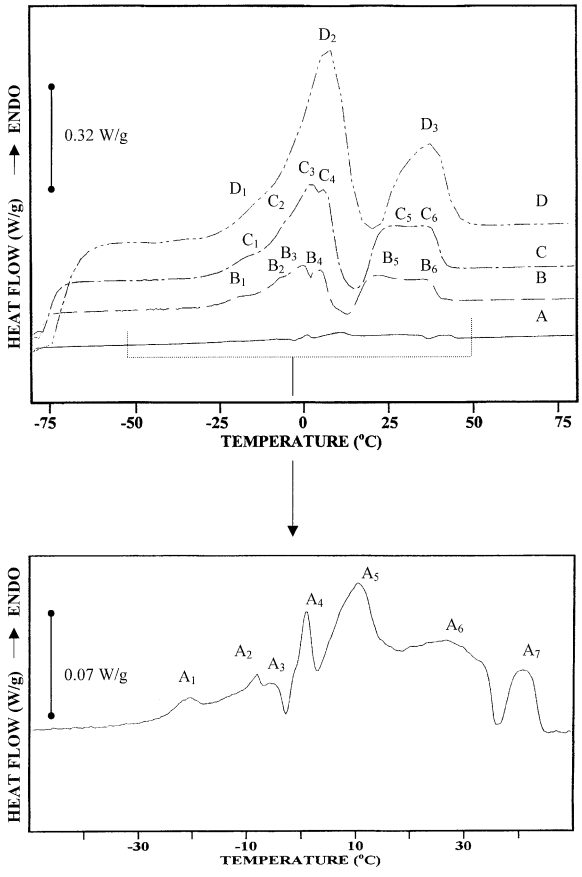

Fig. 4. Differential scanning calorimetry melting curves of refined-bleached-deodorised palm oil (RBDPO) at heating rates varying from 1 to 20 °C/min. Abbreviations: see Fig. 2. Refer to Table 2 for transition temperatures.

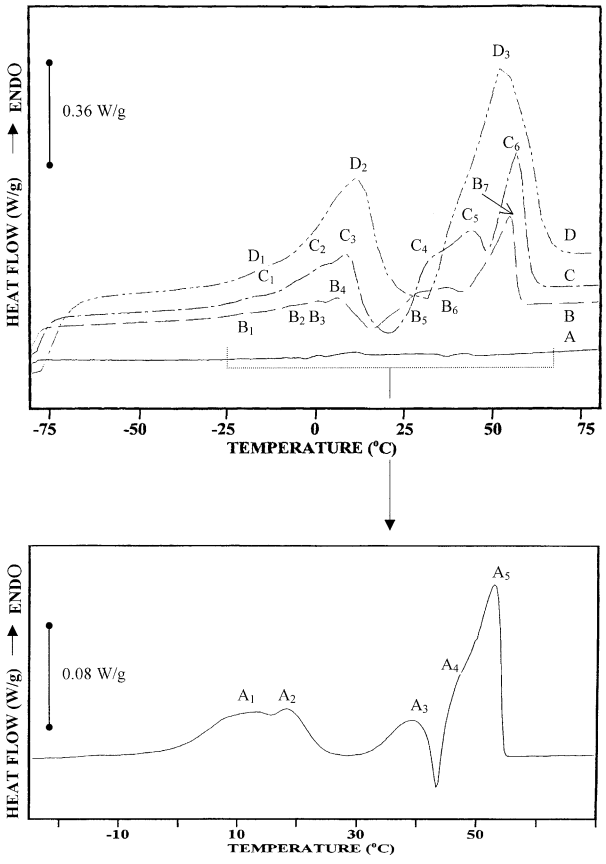

Fig. 5. Differential scanning calorimetry melting curves of refined-bleached-deoderised palm stearin ($RBDPO_s$) at heating rates varying from 1 to 20 °C/min. Abbreviations: see Fig. 2. Refer to Table 2 for transition temperatures.

3.2.3. RBD palm oil (RBDPO)

DSC melting curves of RBDPO and their respective transition temperatures analysed with different heating rates are presented in Fig. 4 and Table 2. Transition for RBDPO with low scanning rate (1 °C/min) was composed of several contiguous peaks resulting from the contribution of a number of TAG components in the oil (Fig. 4, curve A). Increasing the scanning rates to 5, 10, and 20 °C/min resulted in thermal transition with two distinct endotherms. Generally, melting curves of the two characteristic peaks corresponded to endothermic transitions of the olein (low-temperature endotherm) and stearin (high-temperature endotherm) fractions. These results are in accord with those reported by other researchers for palm oil sample (Che Man, Haryati, Ghazali, & Asbi, 1999).

3.2.4. RBD palm stearin (RBDPO$_S$)

DSC melting curves of RBDPO$_S$ at different heating rates have the characteristic profile shown in Fig. 5. The corresponding transition temperatures are presented in Table 2. At 20°C/min, two distinct endotherms with an endothermic trough (exothermic peak) in between these two endotherms were recorded (Fig. 5, curve D). It is widely acknowledged that the lower-

Table 5
Distribution of trisaturated, monounsaturated, diunsaturated and triunsaturated triacylglycerols (TAG) in edible oil samples[a]

Sample	TAG distribution (%)			
	SSS	SSU	SUU	UUU
CtO	86.4±0.74[a]	6.11±0.12[f]	1.32±0.08[f]	0.61±0.08[cd]
PKO	70.25±0.11[b]	16.28±0.12[e]	6.01±0.05[e]	1.40±0.01[d]
RBDPO	9.78±0.08[d]	48.84±0.14[a]	36.54±0.23[c]	4.84±0.02[b]
RBDPO$_{SO}$	2.94±0.06[e]	46.49±0.10[b]	44.94±0.05[b]	5.63±0.02[ab]
RBDPO$_S$	37.66±0.06[c]	42.24±0.20[c]	18.10±0.58[d]	1.90±0.02[c]
RPO$_O$	3.34±0.05[e]	34.55±0.02[d]	55.69±0.06[a]	6.42±0.09[a]

[a] Each value in the table represents the mean standard deviation of triplicate analyses. Means within each column with different superscripts are significantly ($P<0.01$) different. Abbreviations: S represents saturated fatty acids; U represents unsaturated fatty acids; SSS, trisaturated triacylglycerol; SSU, monounsaturated triacylglycerol; SUU, diunsaturated; UUU, triunsaturated triacylglycerol. The sequence does not necessarily reveal that on the glycerine moiety. For other abbreviations see Table 1.

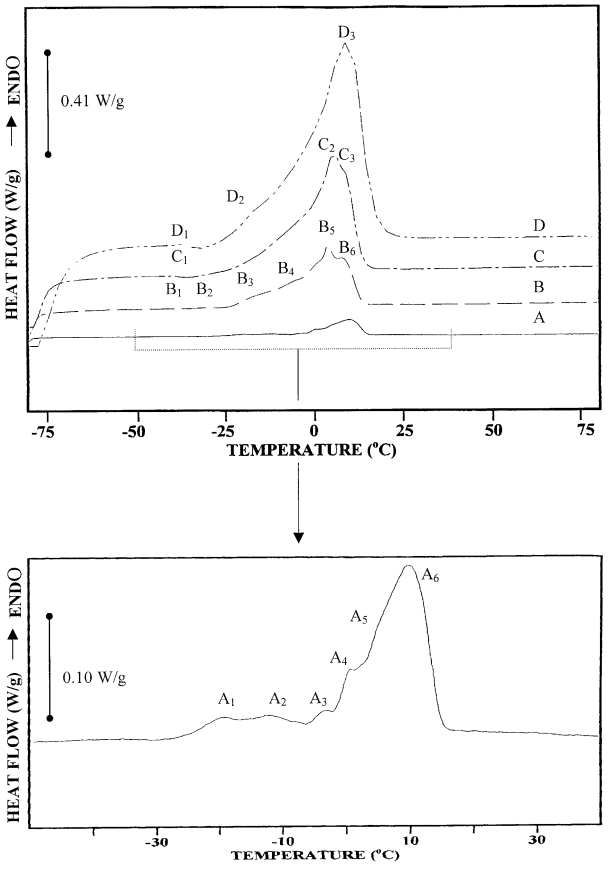

Fig. 6. Differential scanning calorimetry melting curves of refined-bleached-deoderised palm superolein (RBDPO$_{SO}$) at heating rates varying from 1 to 20 °C/min. Abbreviations: see Fig. 2. Refer to Table 2 for transition temperatures.

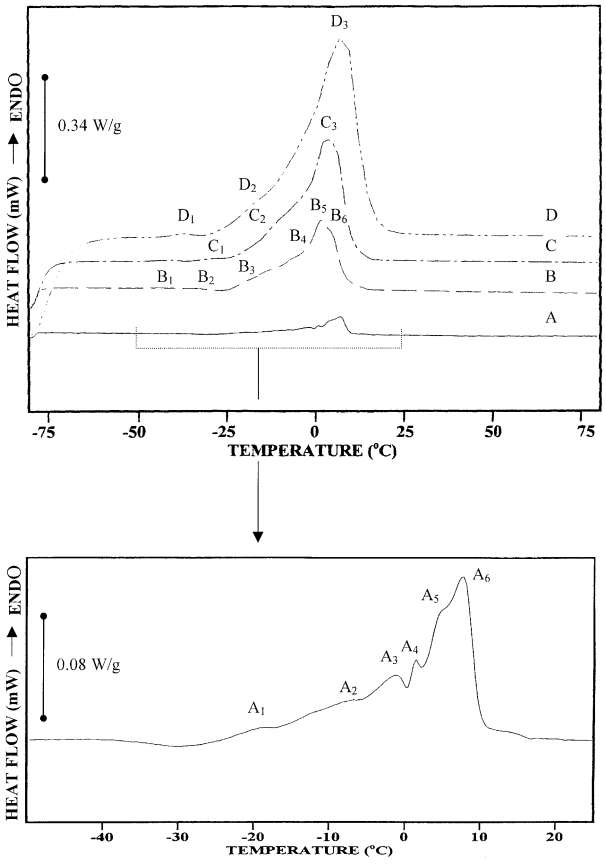

Fig. 7. Differential scanning calorimetry melting curves of red palm olein (RPO$_O$) at heating rates varying from 1 to 20 °C/min. Abbreviations: see Fig. 2. Refer to Table 2 for transition temperatures.

temperature endotherm is caused by a small amount of olein fraction trapped during the fractionation process, while the more prominent higher-temperature endotherm corresponded to the melting of the stearin fraction. Similar DSC melting profiles to the present study were reported by other researchers (Che Man et al., 1999). The lower-temperature endotherm with two or more less-resolved contiguous peaks was also recorded for the $RBDPO_s$ sample scanned at 1, 5 and 10 °C/min, respectively. Overall, the higher-temperature endotherm consisted of one main peak with a small leading shoulder peak on the lower temperature side. This small leading shoulder shifted progressively toward lower temperature and grew into a separate peak as heating rate was decreased. At 1 °C/min, a sharp exotherm valley between these two higher-temperature endotherms indicated that significant structural reorganisation (solid-to-solid transformation) was occurring during the DSC scans (Fig. 5, curve A). The relative narrowness of the endotherm A_5 observed is probably a result of a high degree of cooperativity between highly saturated SSS TAG units (Fig. 5, curve A).

3.2.5. RBD palm olein ($RBDPO_{SO}$) and red palm olein (RPO_O)

The thermal curves for $RBDPO_{SO}$ and RPO_O at different heating rates are given in Figs. 6 and 7, respectively. Their corresponding transition temperatures are given in Table 2. The DSC melting curves in the heating rate studies, in both $RBDPO_{SO}$ and RPO_O samples, exhibited mainly one major melting peak, which corresponded in temperature to the melting of the olein fraction. Multiple-shouldered peaks at lower temperature are observed for the sample scanned at 1 and 5 °C/min, respectively (Figs. 6 and 7, curves A and B). Possibly, at the slow heating rate, there is a greater opportunity for chain rearrangement in the crystallites and thus a smaller fraction will melt at a slow temperature. These shouldered peaks gradually merged with the major melting peak as the heating rate was increased (Figs. 6 and 7, curves C and D). These results would indicate that the olein fraction contributes mainly to the low-temperature transition and that the stearin fraction is responsible for the high-temperature transition. The findings of this study are in agreement with those reported by Che Man et al. (1999).

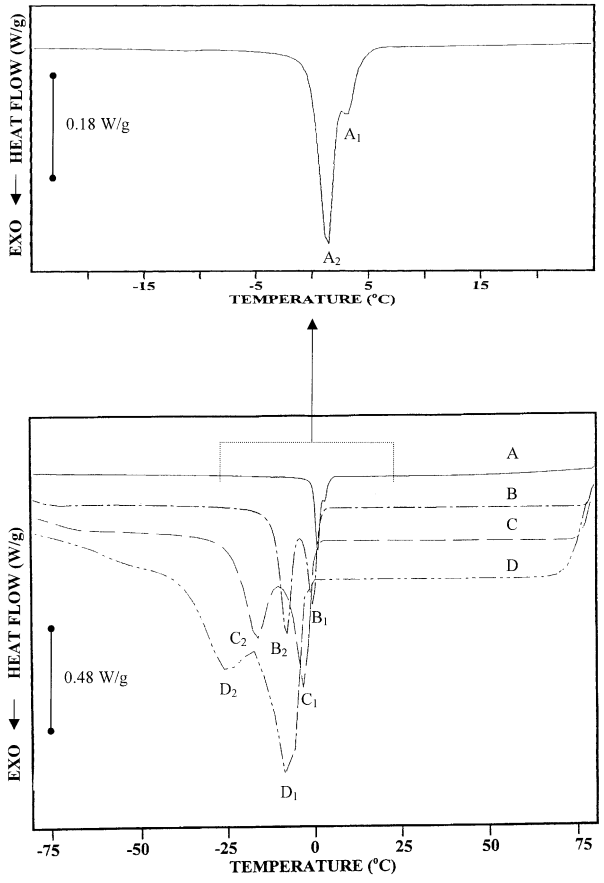

Fig. 8. Differential scanning calorimetry crystallisation curves of coconut oil (CtO) at heating rates varying from 1 to 20 °C/min. Abbreviations: see Fig. 2. Refer to Table 3 for transition temperatures.

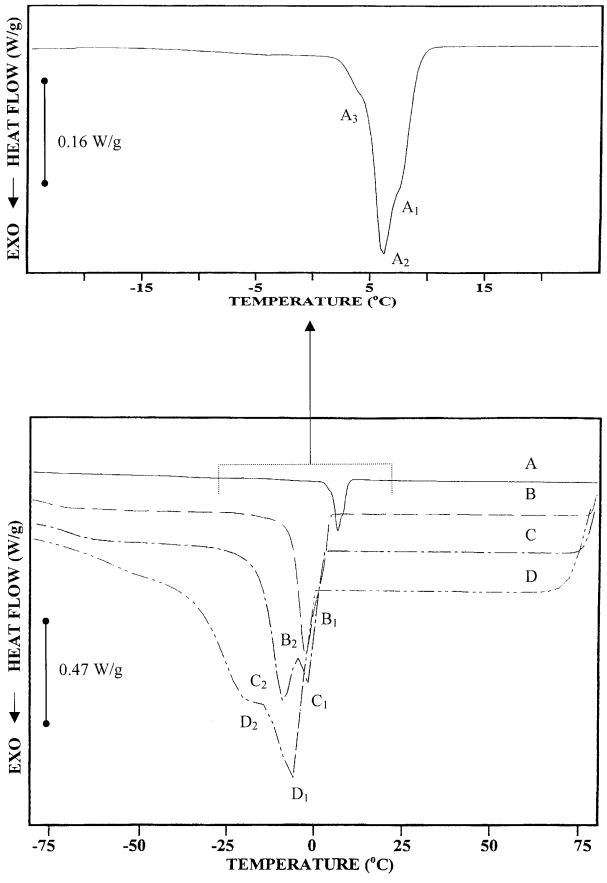

Fig. 9. Differential scanning calorimetry crystallisation curves of palm kernel oil (PKO) at heating rates varying from 1 to 20 °C/min. Abbreviations: see Fig. 2. Refer to Table 3 for transition temperatures.

3.3. Behaviour of oils during the cooling process

When cooled in a DSC, oil samples often exhibit multiple exotherms but they are less complicated than their respective melting curves. The subdivision of the crystallisation curve of oil samples, into different exothermic regions, corresponds to different TAG types. In essence, as the melt is cooled from above the crystallisation temperature of the higher melting TAG component to below the crystallisation temperature of that component, the higher melting component will exhibit more rapid crystallisation. As the crystalline phase is forming, it will have a higher concentration of the TAG component which is kinetically favoured. As the concentration of this TAG component is depleted, the less kinetically favoured TAG component would enter into the crystallisation process until all TAG components crystallised.

The crystallisation process was noticeably affected by the cooling rate. The position and magnitude of the exotherms were dependent on the cooling rate. The crystallisation exotherm shifts to lower temperature as the rate of cooling increases. Also, the breadth of the crystallisation exotherm, on cooling from the melt, increases with increasing cooling rate. Higher cooling rates should also lead to a broader distribution of crystallising temperatures. The breadth of the exotherm is also increased at higher cooling rates, due to the instrumental limitation of the DSC in conducting heat through the sample. As the cooling rate is increased further, the intervals between the three peaks become greater. Since crystallisation takes a finite amount of time, the samples that are cooled quickly will experience a wider temperature range during crystallisation than those that were cooled slowly.

Generally, sample crystallising at slow cooling rates gave more time to allow interactions between TAG. This can be an indication of complete crystallisation of various TAG in the oil to a crystal structure within a narrow temperature ranges. Therefore, the crystallisation of these mixtures of TAG proceeds interactively, which was reflected by the presence of one exotherm. These results are indicative of co-crystallisation. Co-crystallisation composed of the TAG with identical chemical structures may be involved. The co-crystallisation has been proved to be strongly dependent on

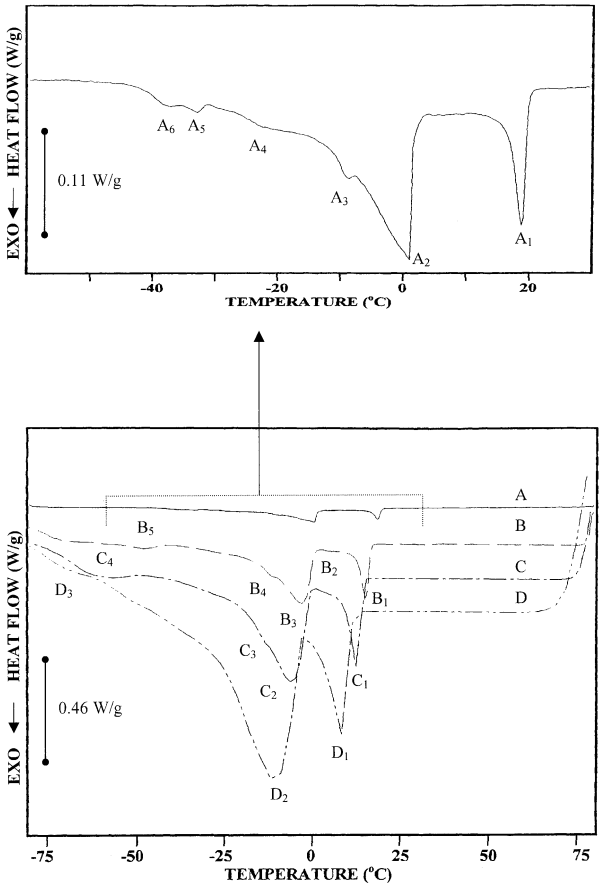

Fig. 10. Differential scanning calorimetry crystallisation curves of refined-bleached-deoderised palm oil (RBDPO) at heating rates varying from 1 to 20 °C/min. Abbreviations: see Fig. 2. Refer to Table 3 for transition temperatures.

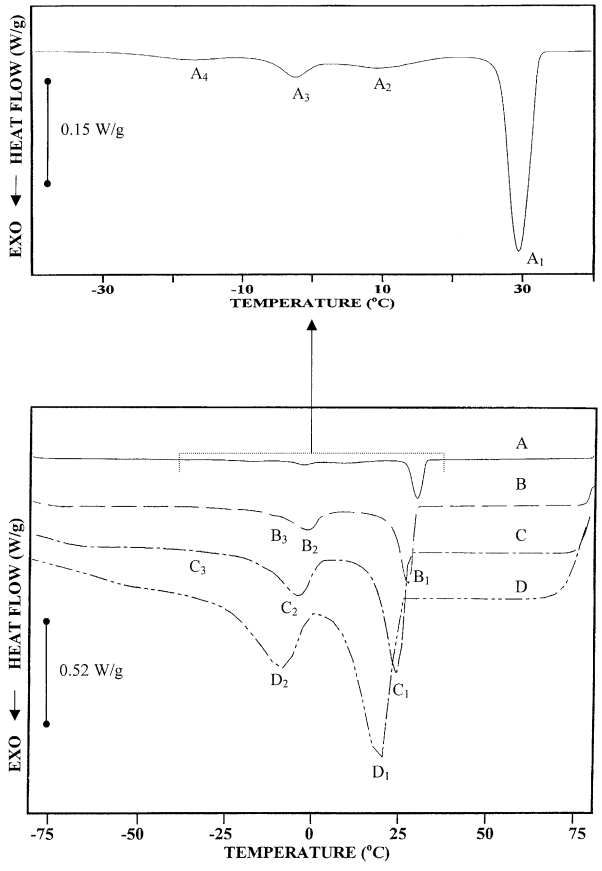

Fig. 11. Differential scanning calorimetry crystallisation curves of refined-bleached-deoderised palm stearin ($RBDPO_S$) at heating rates varying from 1 to 20 °C/min. Abbreviations: see Fig. 2. Refer to Table 3 for transition temperatures.

crystallisation rate. Co-crystallisation seems to be a more reasonable, possibility due to the homogeneity of the TAG components.

3.3.1. Coconut oil (CtO)

The crystallisation curves for CtO samples crystallised at a series of cooling rates are illustrated in Fig. 8. Their corresponding transition temperatures are shown in Table 3. The CtO sample exhibited two overlapping exothermic peaks. As the cooling rate decreased, both exothermic peaks shifted to higher temperatures and finally merged with the lower temperature peak. The height of the higher-temperature peak diminished with the decreasing cooling rate, and the peak almost essentially disappeared at 1 °C/min, whereas the height of the lower-temperature peak increased with decreasing cooling rate. At the same time, the location of the crystallising peaks shifted to higher temperatures. One possible explanation for the disappearance of the higher-temperature crystallisation peak at low cooling rate was the stronger co-crystallisation effect of TAG in the CtO as compared with higher cooling rates.

3.2.2. Palm kernel oil (PKO)

Fig. 9 illustrates the stacked DSC curves for the crystallisation of the PKO at various cooling rates. Their corresponding transition temperatures are listed in Table 3. Generally, the crystallisation curves of PKO consisted of two overlapped exotherms. The relative size of both exotherms can be manipulated by controlling the cooling rate of samples. As the cooling rate decreases, the lower-temperature exotherm increases in size and is superimposed on the lower-temperature tail of higher-temperature exotherm. There was a considerable overlap of peak areas at slow cooling rates. At scan rates of 5, 10, and 20 °C/min, the crystallisation trace consistently exhibited two overlapped exotherms (Fig. 9, curves B–D), whereas at 1 °C/min, the crystallisation trace showed two overlapped exotherms with one slight shoulder exotherm (Fig. 9, curve A). The much smaller exotherm was noted on the lower temperature side. The two overlapped exotherms are thus probably due to the crystallisation of five major trisaturated (SSS) TAG present in PKO, namely CLaLa, LaLaLa, LaLaM, LaMM, which accounted for almost 64% of the total TAG (Table 3a and 4).

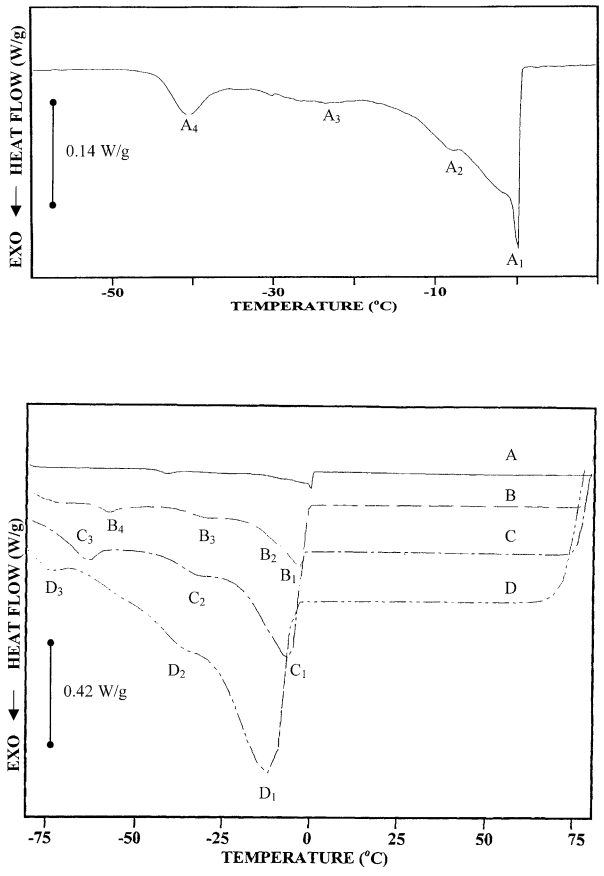

Fig. 12. Differential scanning calorimetry crystallisation curves of refined-bleached-deoderised palm superolein ($RBDPO_{SO}$) at heating rates varying from 1 to 20 °C/min. Abbreviations: see Fig. 2. Refer to Table 3 for transition temperatures.

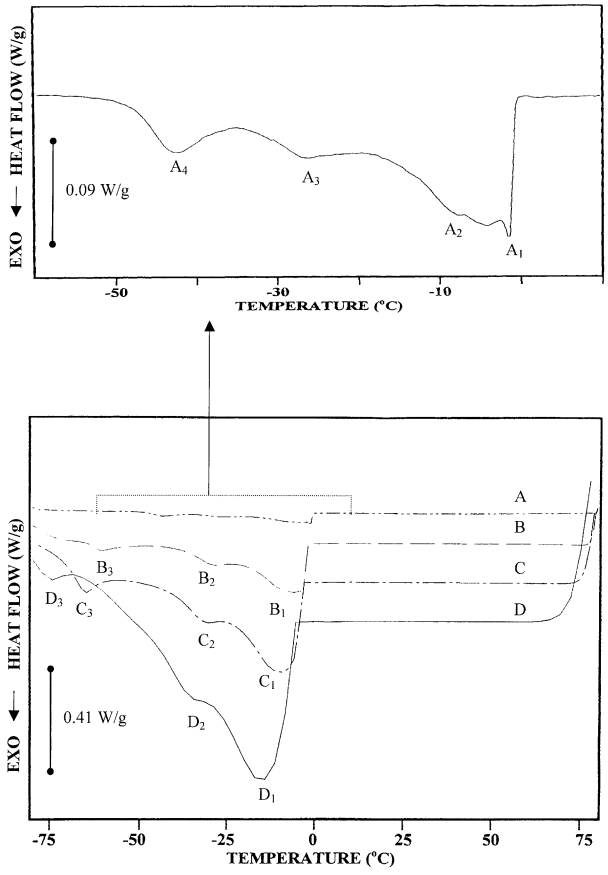

Fig. 13. Differential scanning calorimetry crystallisation curves of red palm olein (RPO_O) at heating rates varying from 1 to 20 °C/min. Abbreviations: see Fig. 2. Refer to Table 3 for transition temperatures.

3.3.3. RBD palm oil (RBDPO)

DSC crystallisation curves for the $RBDPO_O$ and their respective transition temperatures at different cooling rates are shown in Fig. 10 and Table 3, respectively. In general, two distinct peaks were observed in the crystallisation behaviour, one corresponding to the peak found in the high temperature (0–20 °C) region and a second at a slightly lower-temperature in the −25–0 °C region. The peak occurring at the higher temperature is sharper. The higher temperature exotherm corresponded to the crystallisation of the stearin fraction while the lower temperature exotherm was attributed to the crystallisation of the olein fraction. At a cooling rate of 1 °C/min, two small overlapping peaks (A_5 and A_6) were observed in the low temperature region (Fig. 10, curve A). With the increase in cooling rate, they merged, increased in size and shifted to lower temperature (Fig. 10, curves B–D).

3.3.4. RBD palm stearin

Fig. 11 depicts the crystallisation curves for the $RBDPO_S$ at various cooling rates. The corresponding transition temperatures are shown in Table 3. The DSC crystallisation curves of the $RBDPO_S$ exhibited a minor exothermic peak at −25–0C in addition to the major exothermic peak at higher temperatures (15–30 °C). When the cooling rate was decreased, more crystallisation occured at higher temperatures during cooling; consequently, the major exothermic peak became larger than the lower-temperature minor exothermic peak. The exothermic peak observed on the DSC curve can be attributed to the transition from crystallisation of the stearin fraction (major exotherm) and some small amount of olein fraction (minor exotherm). As cooling rate decreased, components of lower temperature peaks increased and smaller differences were found between amounts of components with higher and lower temperature peaks.

3.3.5. RBD palm superolein ($RBDPO_{SO}$) and red palm olein (RPO_O)

The DSC crystallisation curves of $RBDPO_{SO}$ and RPO_O at different heating rates are shown in Figs. 12 and 13, respectively. The respective transition temperatures are given in Table 3. The crystallisation curves of both oils showed one distinct exothermic peak with two/three overlapping shoulder peaks. The position and breadth of the crystallisation exotherms upon cooling from melt showed that, as the cooling rate was increased, the distribution of melting temperatures broadened and shifted to lower temperatures. Multiple-shouldered peaks at lower temperature were observed for the sample scanned at 1 and 5 °C/min, respectively (Figs. 12 and 13, curves A and B). The crystallisation curves of $RBDPO_{SO}$ and RPO_O were quite similar except that the temperature of the crystallisation peaks of RPO_O was slightly lower than that of $RBDPO_{SO}$.

3.4. Changes in enthalpy, offset- and onset-temperatures

In consideration of the above discussion and analysis, it seems that the origins of the multiple peaks for a particular oil sample need to be determined on a case-to-case basis. Therefore, coherent overall conclusions have yet to be drawn. However, in nearly all the cases, the melting endotherms or crystallisation exotherms correspond to the melting or crystallisation of the major TAG fractions present in the oil. Although the above results are very informative, if considered on no more than a comparative basis, it is clearly advantageous to be able to discuss them in terms of absolute characterisation and simple identification of edible oils, more especially because they may shed light on the difficult problem of classification. As a corollary it seems that melting and crystallisation curves of CtO and palm oil and palm-based products differ considerably in terms of their extrapolated offset-temperature (T_{off}) and onset-temperature (T_{on}), respectively (Table 6). Differences in onset temperature (melting transition) and offset-temperature (crystallisation transition) for all oils could not be determined because no concluding baseline was observed in most of the oil samples. We were using the T_{off} and T_{on} computed by the DSC instrument instead of the manually marked offset or onset temperature, because the latter value might give misleading results due to the irregular shape of some endothermic peaks. The change in heating rate had a great effect on the T_{off}. Generally, there was a shift of T_{off} toward higher values with increasing heating rates (Table 6), although some variation from this order was found, depending on the type of oil samples. This is well expected since the oil system has no time to respond to the fast heating rate. For each type of oil sample, the T_{off} values obtained at a heating rate of 20 °C/min were significantly ($P<0.01$) highest among all heating rates used in this study (Table 6). For all oil samples, statistically significant ($P<0.01$) differences in the T_{off} were seen at all scanning rates (Table 6). The onset temperatures (T_{on}) at different cooling rates are also presented in Table 6. The T_{on} increased with rises in cooling rates. Conversely, for all oil samples, statistically significant differences ($P<0.01$) were seen at 1 and 5 °C/min (Table 6).

In Table 6, the coefficients of variation (CV) for the T_{off} and T_{on} values of all oil samples at four different scanning rates are presented for comparison. The results reveal excellent reproducibility for determination of the T_{off} and T_{on} values. The oil samples were evaluated in replicates of four and the CV was always lower than 10% (except for two extremely low mean values of T_{on}).

Table 6
Comparison of differential scanning calorimetry-measured offset temperature for four different heating rates of edible oil samples[a]

Sample	Temperature (°C)							
	1/min		5/min		10/min		20/min	
	Mean±S.D.	CV (%)	Mean±S.D.	CV (%)	Mean±S.D.	CV (%)	Mean±S.D.	CV (%)
Melting (offset)								
CtO	$22.39\pm0.71^{d}_{D}$	3.16	$25.30\pm0.02^{d}_{C}$	0.06	$28.10\pm0.08^{d}_{B}$	0.30	$34.41\pm1.03^{d}_{A}$	2.98
PKO	$25.87\pm0.09^{c}_{D}$	0.36	$28.98\pm0.01^{c}_{C}$	0.02	$32.18\pm0.72^{c}_{B}$	2.24	$39.80\pm0.86^{c}_{A}$	2.17
RBDPO	$44.73\pm0.19^{b}_{B}$	0.43	$40.59\pm0.46^{b}_{D}$	1.13	$42.37\pm0.64^{b}_{C}$	1.52	$47.12\pm0.47^{b}_{A}$	1.01
$RBDPO_{SO}$	$15.16\pm0.31^{f}_{B}$	2.05	$13.86\pm0.25^{e}_{B}$	1.83	$14.92\pm0.72^{e}_{B}$	4.83	$18.73\pm0.57^{e}_{A}$	3.02
$RBDPO_{S}$	$54.83\pm0.05^{a}_{D}$	0.09	$57.78\pm0.65^{a}_{C}$	1.13	$62.17\pm1.27^{a}_{B}$	2.04	$68.02\pm0.35^{a}_{A}$	0.52
RPO_{O}	$17.07\pm0.13^{e}_{A}$	0.79	$9.64\pm0.16^{f}_{C}$	1.62	$14.15\pm0.06^{e}_{B}$	0.40	$16.63\pm0.91^{f}_{A}$	5.49
Crystallisation (onset)								
CtO	$5.1\pm0.0^{d}_{A}$	0.6	$2.1\pm0.0^{d}_{B}$	0.0	$0.6\pm0.1^{d}_{C}$	10.0	$-1.8\pm0.3^{d}_{D}$	−13.9
PKO	$9.5\pm0.0^{c}_{A}$	0.2	$4.4\pm0.4^{c}_{B}$	9.9	$2.9\pm0.0^{c}_{C}$	0.8	$-0.1\pm0.0^{c}_{D}$	−6.4
RBDPO	$20.2\pm0.1^{b}_{A}$	0.2	$17.0\pm0.3^{b}_{B}$	1.7	$15.8\pm0.1^{b}_{C}$	0.9	$12.8\pm0.6^{b}_{D}$	4.5
$RBDPO_{SO}$	$0.9\pm0.0^{e}_{A}$	2.1	$-0.5\pm0.0^{e}_{B}$	−9.3	$-1.6\pm0.1^{e}_{C}$	−4.2	$-4.3\pm0.4^{e}_{D}$	−10.0
$RBDPO_{S}$	$33.0\pm0.7^{a}_{A}$	2.0	$29.7\pm0.2^{a}_{B}$	0.6	$27.6\pm0.2^{a}_{C}$	0.5	$25.3\pm0.9^{a}_{D}$	3.4
RPO_{O}	$-0.4\pm0.0^{f}_{A}$	−8.5	$-1.8\pm0.2^{f}_{B}$	−8.5	$-2.0\pm0.0^{e}_{B}$	−2.2	$-5.1\ 0.0^{e}_{C}$	−0.2

[a] Each value in the table represents the mean ± standard deviation of four determinations. Means within each column with different superscripts are significantly ($P<0.01$) different. Means within each row with different subscript are significantly ($P<0.01$) different. Abbreviations: S.D., standard deviation; CV, coefficient of variation. For other abbreviations see Table 1.

The melting and crystallisation enthalpies of all oil samples are shown in Table 7. The results of the statistical test (Duncan's multiple-range test), comparing the mean difference among these data, are also shown in Table 7. The oil samples were evaluated in replicates of four and the CV was always lower than 7%. Generally, the oil samples with high degrees of saturation (CtO, PKO and $RBDPO_S$) showed DSC melting enthalpies at higher values than the oil sample with a high degree of unsaturation (RBDPO, $RBDPO_{SO}$ and RPO_O). This observation is predictable since the oil sample with a higher degree of saturation requires more energy during the melting process. The oil samples showed DSC crystallization enthalpies in between −74 and −118 J/g (Table 7). In the industrial fractionation of vegetable oils and fats, it is an important aim of the process to limit this exotherm by varying the rate of heat removal and agitation with temperature (Timms, 1995).

Several difficulties may be encountered in enthalpy determination. Two of special importance are: (1) the baseline for the melting curve may not be horizontal, and (2) the peak is not generally symmetrical. The baseline of DSC curves is often different before and after a peak, due to changes in the physical properties of the sample during the reaction which produces the peak, and thus it is difficult to determine the baseline to be used for enthalpy determination (especially at high scanning rates such as 10 and 20 °C/min). The baseline problem is always a source of uncertainty in DSC, especially in the measurement of enthalpy. Therefore, interpretation of enthalpy, based on such DSC curves, must be done with caution.

Table 7
Comparison of differential scanning calorimetry-measured melting and cooling enthalpies of edible oil samples at 1 °C/min[a]

Sample	Enthalpy (J/g)	
	Mean±S.D.	CV (%)
Melting		
CtO	120.6 ± 2.0^{b}	1.7
PKO	114.1 ± 2.2^{c}	1.9
RBDPO	86.3 ± 0.9^{d}	1.1
$RBDPO_{SO}$	78.4 ± 1.7^{e}	2.2
$RBDPO_{S}$	130.6 ± 8.1^{a}	6.2
RPO_{O}	79.5 ± 0.2^{e}	0.3
Crystallisation		
CtO	-106.5 ± 1.5^{c}	−1.2
PKO	-104.0 ± 0.8^{c}	−0.8
RBDPO	-92.9 ± 3.5^{b}	−3.8
$RBDPO_{SO}$	-77.4 ± 1.4^{a}	−1.8
$RBDPO_{S}$	-117.5 ± 0.4^{d}	−0.3
RPO_{O}	-74.7 ± 1.4^{a}	−1.9

[a] Each value in the table represents the mean ± standard deviation of four determinations. Means within each column with different superscripts are significantly ($P<0.01$) different. Abbreviations: see Tables 1 and 6.

The results obtained from the present study show that, if calorimetric criteria are appropriately established, DSC is an efficient method for characterising edible oils. Their characterisation can be useful in

identifying edible oils and fats. We conclude that accurate comparisons of the calorimetric experiments in the edible oils can only be done when these DSC experiments are carried out at the same scanning rate. The use of slow scan rates is advisable in that it minimises instrumental lag in output response and, at a given temperature, the reaction being examined is closer to chemical equilibrium, as well as giving the true line shape of the transition which will be important if identification of the data is to be undertaken. Consequently, a relatively low scanning rate (e.g. 1 or 5 °C/min) is required to ensure thermal equilibrium of the sample at the time of data collection. In general, a study of the melting/crystallisation curves of any one oil/fat could distinguish it from any of the other five.

Acknowledgements

This research work was supported by Universiti Putra Malaysia (IRPA Project No. 03-02-04-003).

References

Anon. (1995). *7 Series/UNIX DSC7 Users Mannual, Version 4.0*. Norwalk, CT, USA: Perkin-Elmer Corporation.

AOCS (1993). *Official methods and recommended practices of the American oil Chemists' Society* (4th ed.). D. Firestone (Ed.), Champaigne, IL: American Oil Chemists' Society.

Breitschuh, B., & Windhab, E. J. (1996). Direct measurement of thermal fat crystal properties for milk-fat fractionation. *Journal of the American Oil Chemists' Society*, *73*, 1603–1610.

Cebula, D. J., & Smith, K. W. (1991). Differential scanning calorimetry of confectionery fats. Pure triglycerides: effects of cooling and heating rate variation. *Journal of the American Oil Chemists' Society*, *68*, 591–595.

Che Man, Y. B., Haryati, T., Ghazali, H. M., & Asbi, B. A. (1999). Composition and thermal profile of crude palm oil and its products. *Journal of the American Oil Chemists' Society*, *76*, 215–220.

deMan, J. M., & deMan, L. (1994). Differential scanning calorimetry techniques in the evaluation of fats for the manufacture of margarine and shortening. *INFORM*, *5*, 522.

Desmedi, A., Culot, C., Deroanne, C., Durant, F., & Gibon, V. (1990). Influence of *cis* and *trans* double bonds on the thermal and structural properties of monoacid triglycerides. *Journal of the American Oil Chemists' Society*, *67*, 653–660.

Dollimore, D. (1996). Thermal analysis. *Analytical Chemistry*, *68*(10), 63R–71R.

Herrera, M. L., Segura, J. A., & Rivarola, G. J., & Añón, M. C. (1992). Relationship between cooling rate and crystallisation behaviour of hydrogenated sunflowerseed oil. *Journal of the American Oil Chemists' Society*, *69*, 898–905.

Ma, C.-Y., Harwalkar, W. R., & Maurice, T. J. (1990). Instrumentation and techniques of thermal analysis in food research. In V. R. Harwalkal, & C.-Y. Ma (Eds.), *Thermal analysis of foods* (pp. 1–15). New York: Elsevier Science Publishing Inc.

SAS. (1989). *Statistical analysis system user's guide: basic statistics*. Cary, NC: SAS Institute.

Sato, K. (1999). Solidification and phase transformation behavior of food fats—a review. *Fett/Lipid*, *12*, 467–474.

Tan, C. P., & Che Man, Y. B. (1999a). Differential scanning calorimetric analysis for monitoring the oxidation of heated oils. *Food Chemistry*, *67*, 177–184.

Tan, C. P., & Che Man, Y. B. (1999b). Quantitative differential scanning calorimetric analysis for determining total polar compounds in heated oils. *Journal of the American Oil Chemists' Society*, *76*, 1047–1057.

Tan, C. P., & Che Man, Y. B. (2000). Differential scanning calorimetry analysis of edible oils: comparison of thermal properties and chemical composition. *Journal of the American Oil Chemists' Society*, *77*, 143–155.

Timms, R. E. (1995). Crystallisation of fats. In R. J. Hamilton (Ed.), *Developments in oils and fats* (pp. 204–223). London: Chapman and Hall.